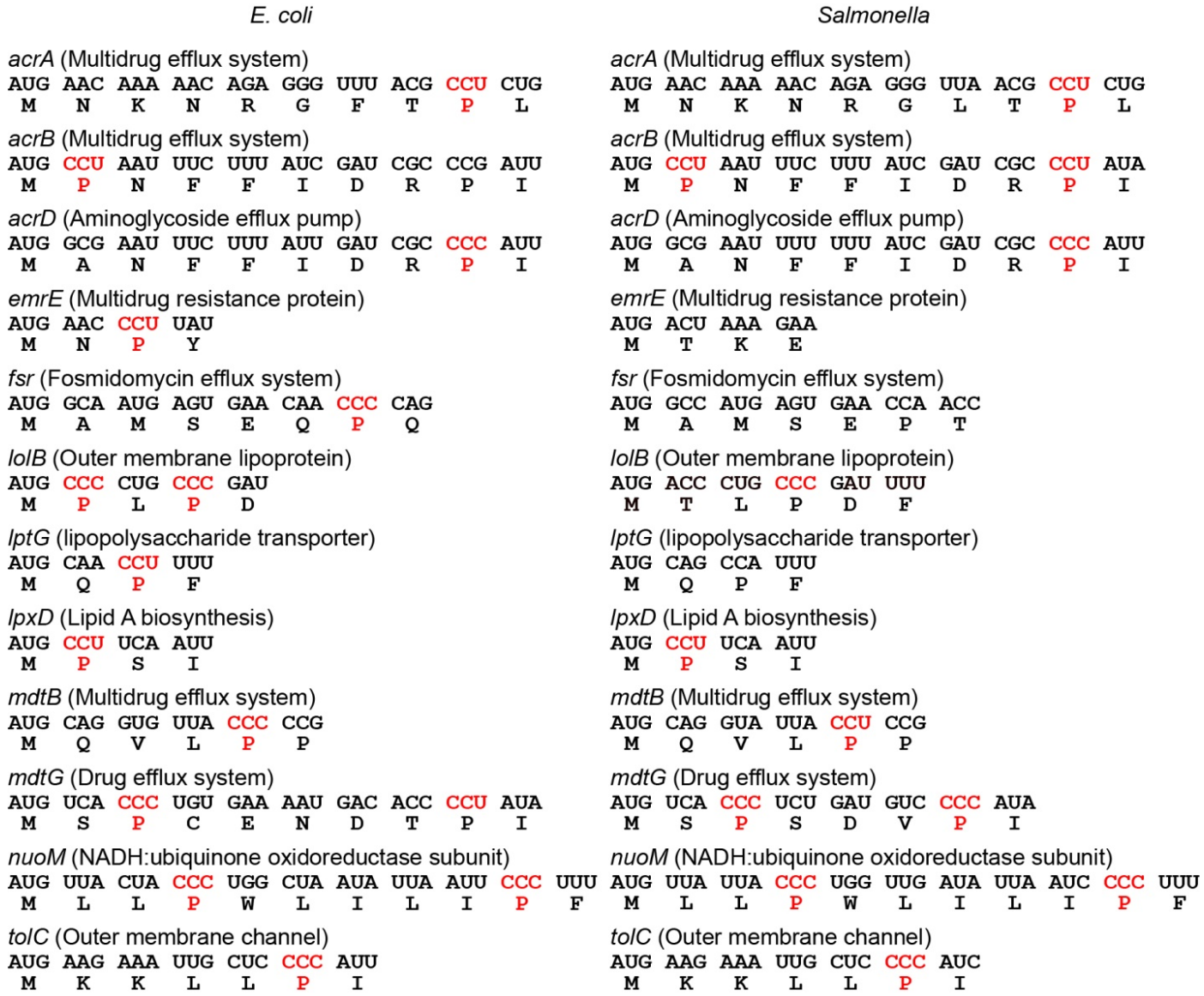


**Figure S1 (Related to Figure 1). The CC[C/U] codon occurs near the initiation codon of Gram-negative membrane-associated genes.** Sequences of selected membrane-associated genes in *E. coli* and *Salmonella* up to the first 15 codons, showing CC[C/U] codons in red.

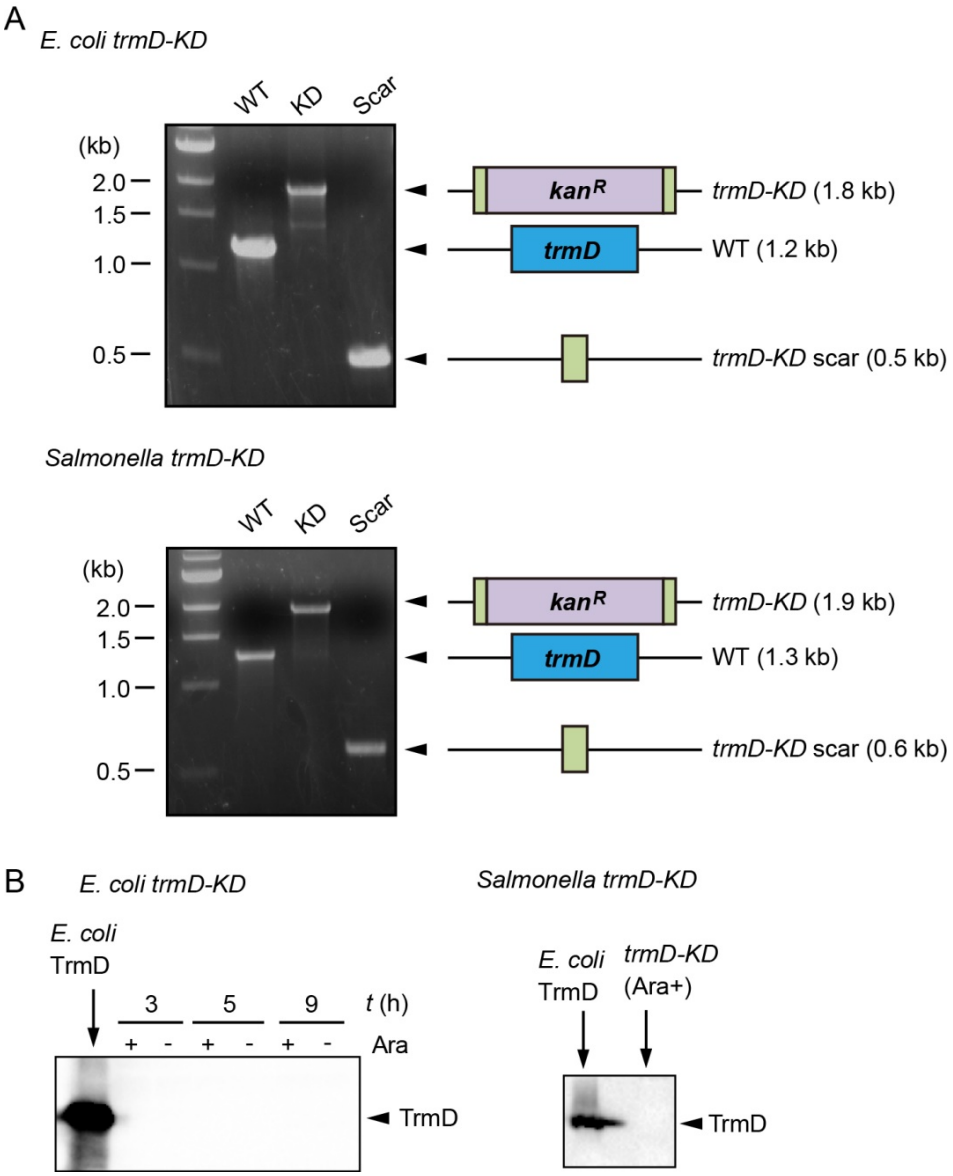


**Figure S2 (Related to Figure 1). Validation of *trmD-KD* strain construction.** **(A)** The chromosomal *trmD* loci from *E. coli* (top) and *Salmonella* (bottom) were amplified via PCR using primers hybridized to the *trmD*-flanking regions. *trmD-KD* cells were constructed via λ-Red recombination, replacing the entire *trmD* sequence with a *kan*$^R$ marker. The marker was subsequently removed with FLP recombinase encoded in pCP20, converting the locus into a scar sequence. **(B)** *E. coli trmD-KD* cells maintained with human Trm5 were grown in Ara+ or Ara− conditions for the indicated time period. Western blotting of whole-cell lysates with antibodies against *Salmonella* TrmD, along with the loading control of purified *E. coli* TrmD, showed no trace of the protein. Whole-cell lysates from *Salmonella trmD-KD* cells grown to mid-log phase also showed no trace of the protein.

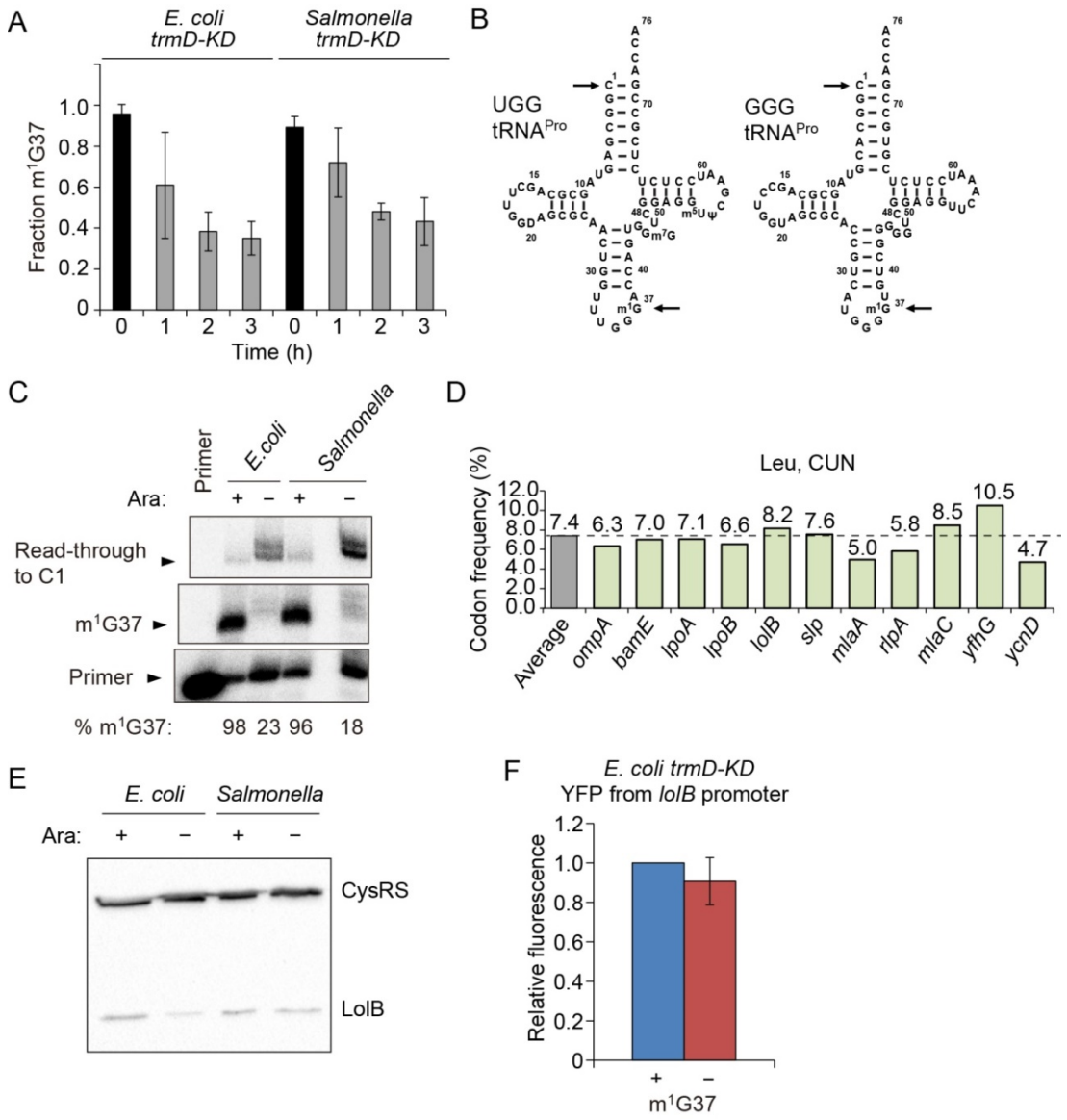


**Figure S3 (Related to Figure 2). m$^1$G37-tRNA levels are decreased over time in *E. coli* and *Salmonella trmD-KD* cells.** **(A)** Levels of m$^1$G37 decreased during pre-depletion of *E. coli trmD-KD* and *Salmonella trmD-KD* cells. Overnight cultures were diluted 1:100 into fresh LB without arabinose (Ara) and grown at 37 °C to deplete pre-existing Trm5 protein and m$^1$G37-tRNAs. At 0, 1, 2, and 3 h after inoculation, the fraction of tRNA$^{Pro/UGG}$ containing m$^1$G37 was determined via primer extension using a primer specific for the UGG isoacceptor (Figure 1F; STAR Methods). **(B)** Sequences and cloverleaf structures of isoacceptor tRNA$^{Pro/UGG}$ and tRNA$^{Pro/GGG}$ of *E. coli*. The m$^1$G37 positions and the first nucleotide C1 are indicated by an arrow. **(C)** m$^1$G37 levels in the absence of Ara are low for the GGG isoacceptor of *E. coli* and *Salmonella* tRNA$^{Pro}$. Gel analysis of primer extension of *E. coli* tRNA indicated stoppage at m$^1$G37 at 23% vs. 98% in the Ara– vs. Ara+ condition. Gel analysis of primer extension of *Salmonella* tRNA indicates stoppage at m$^1$G37 at 18% vs. 96% in the Ara– vs. Ara+ condition. **(D)** Leu codon CUN usage of genes encoding *E. coli* outer-membrane proteins that showed reduced abundance in the membrane proteomic analysis in the Ara– vs. Ara+ condition. Relative to the average CUN codon usage in *E. coli* (7.4%), these genes for outer-membrane proteins do not show abundance of the codon, indicating that the reduction of their protein abundance is not correlated with CUN codon usage. **(E)** Western blotting analysis showed that protein level of LolB is decreased relative to CysRS in Ara– vs. Ara+ cells of *E. coli* and *Salmonella*. **(F)** Transcription from the *E. coli lolB* promoter was similar in m$^1$G37+ and m$^1$G37– conditions (where m$^1$G37– indicates m$^1$G37 deficiency), using YFP as the reporter (STAR Methods). Signal intensity was normalized to cell density in each condition. The expression level and error bars in m$^1$G37+ vs. m$^1$G37– cells are the mean ± SD, n = 3.

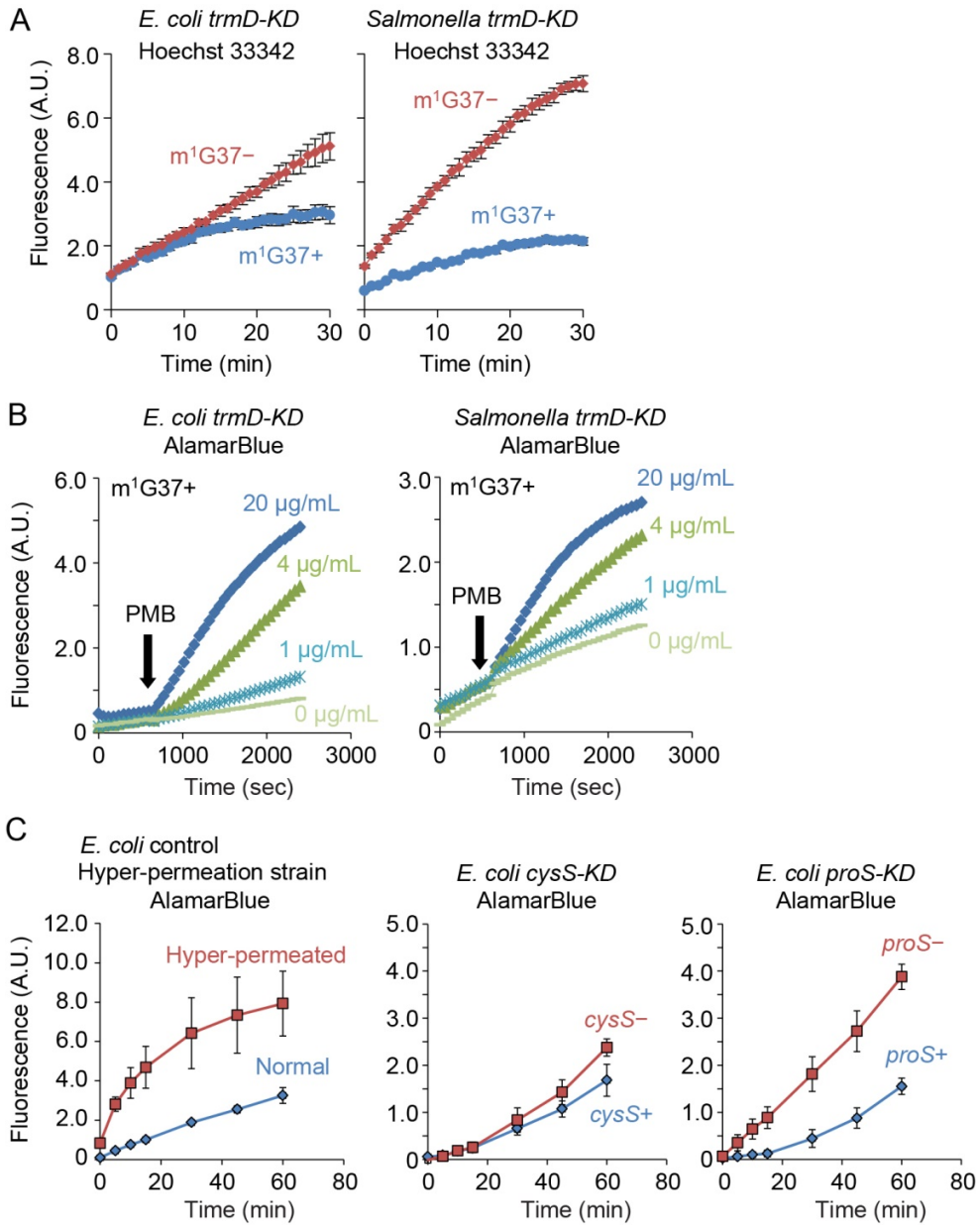


**Figure S4 (Related to Figure 3). *E. coli trmD-KD* cells and *Salmonella trmD-KD* cells show higher membrane permeability to AlamarBlue and Hoechst 33242 in m$^1$G37-deficient vs. m$^1$G37+ conditions.** **(A)** In addition to AlamarBlue, Hoechst 33342 dye was also used for permeability assay. Levels of intracellular accumulation of the dye are shown over time. Data and error bars are mean ± SD, n = 3, and m$^1$G37− indicates m$^1$G37-deficient cells. Both *E. coli trmD-KD* (left) and *Salmonella trmD-KD* (right) showed higher uptake of the dye in the m$^1$G37− relative to the m$^1$G37+ condition. **(B)** Polymyxin B permeabilizes the cell membrane to promote dye accumulation. *E. coli trmD-KD* (left) and *Salmonella trmD-KD* (right) were grown in the m$^1$G37+ condition and the uptake of AlamarBlue was monitored for 10 min. Polymyxin B was then added at the indicated concentrations and the dye uptake was monitored over the next 30 min. Data show a dose-dependent uptake of AlamarBlue. **(C)** Faster uptake of AlamarBlue in membrane-permeabilized cells. A hyper-permeable strain (Krishnamoorthy *et al*, 2016), expressing a mutant of the outer membrane FhuA pore protein, was used for AlamarBlue accumulation assay (left). Cells with FhuA over-expression (defective outer membrane, red) showed faster uptake of the dye compared to a condition without over-expression (normal membrane, blue). *E. coli cysS-KD* (middle) and *proS-KD* (right) cells were used for the accumulation assay; when depleted of the respective protein product (red), faster uptake of the dye was observed compared to the non-depleted condition (blue) for the *proS-KD* strain but not for the *cysS-KD* strain. Data and errors bars are mean ± SD, n = 3.

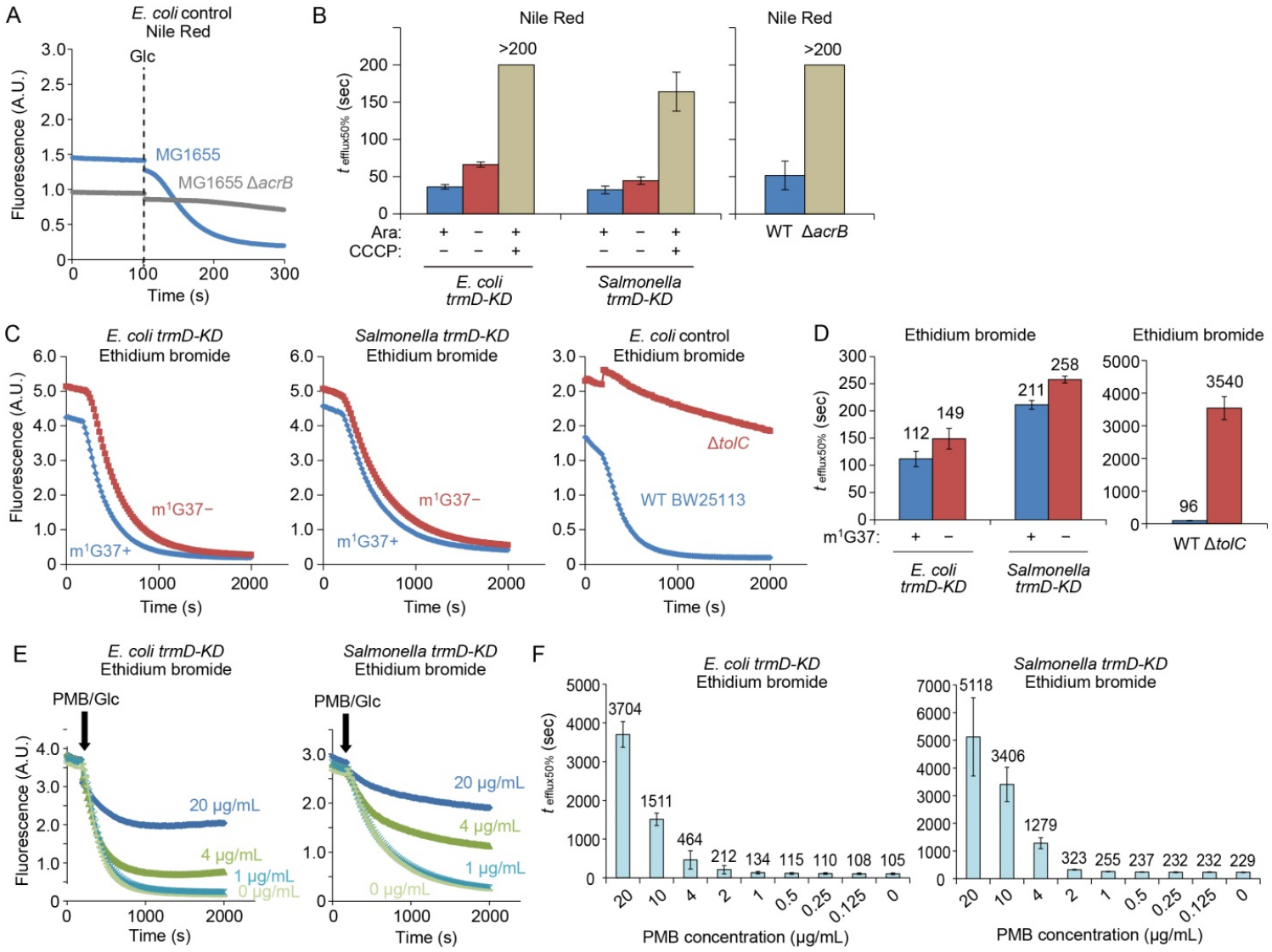


**Figure S5 (Related to Figure 3): *E. coli trmD-KD* and *Salmonella trmD-KD* cells show less efflux of Nile Red in m$^1$G37-deficient vs. m$^1$G37+ conditions.** **(A and B)** Control experiment for Nile Red assay in Figure 3C-3E. The lack of efflux in m$^1$G37+ cells in the presence of CCCP and in MG1655 Δ*acrB* cells served as negative controls, while the efflux of Nile Red by wild-type MG1655 cells served as a positive control (A). The full data set for $t_{efflux\ 50\%}$ measurements as in Figure 3E is shown in (B). Errors are mean ± SD, n = 3, and m$^1$G37– indicates m$^1$G37 deficiency. **(C and D)** In addition to Nile Red, ethidium bromide (EtBr) was used to investigate efflux activity. *E. coli trmD-KD* (C, left) and *Salmonella trmD-KD* (C, middle) were grown in m$^1$G37+ or m$^1$G37-deficient conditions, and cells were washed and incubated in Nile Red buffer with 50 μM CCCP and 10 μg/mL EtBr for pre-loading for 2 h at 30 °C. Cells were washed and the EtBr fluorescence was monitored over 3 min, then efflux was activated by the addition of 50 mM glucose, followed by fluorescence measurements for 30 min. *E. coli* BW25113 wild-type and Δ*tolC* strains were used as controls (C, right). $t_{efflux\ 50\%}$ is summarized in (D). Data and error bars are mean ± SD, n = 3, and m$^1$G37− indicates m$^1$G37 deficiency. **(E and F)** Polymyxin B inactivates the efflux system. *E. coli trmD-KD* (E, left) and *Salmonella trmD-KD* (E, right) were grown in the m$^1$G37+ condition and processed as in (C). After the initial 3 min fluorescence measurement, polymyxin B was added at the indicated concentrations and cells were incubated at room temperature for 5 min. Efflux was then activated by the addition of 50 mM glucose, followed by fluorescence measurements for 30 min. $t_{efflux\ 50\%}$ is summarized in (F) and the data show reduced efflux activity in a dose-dependent manner. Data and error bars are mean ± SD, n = 3.

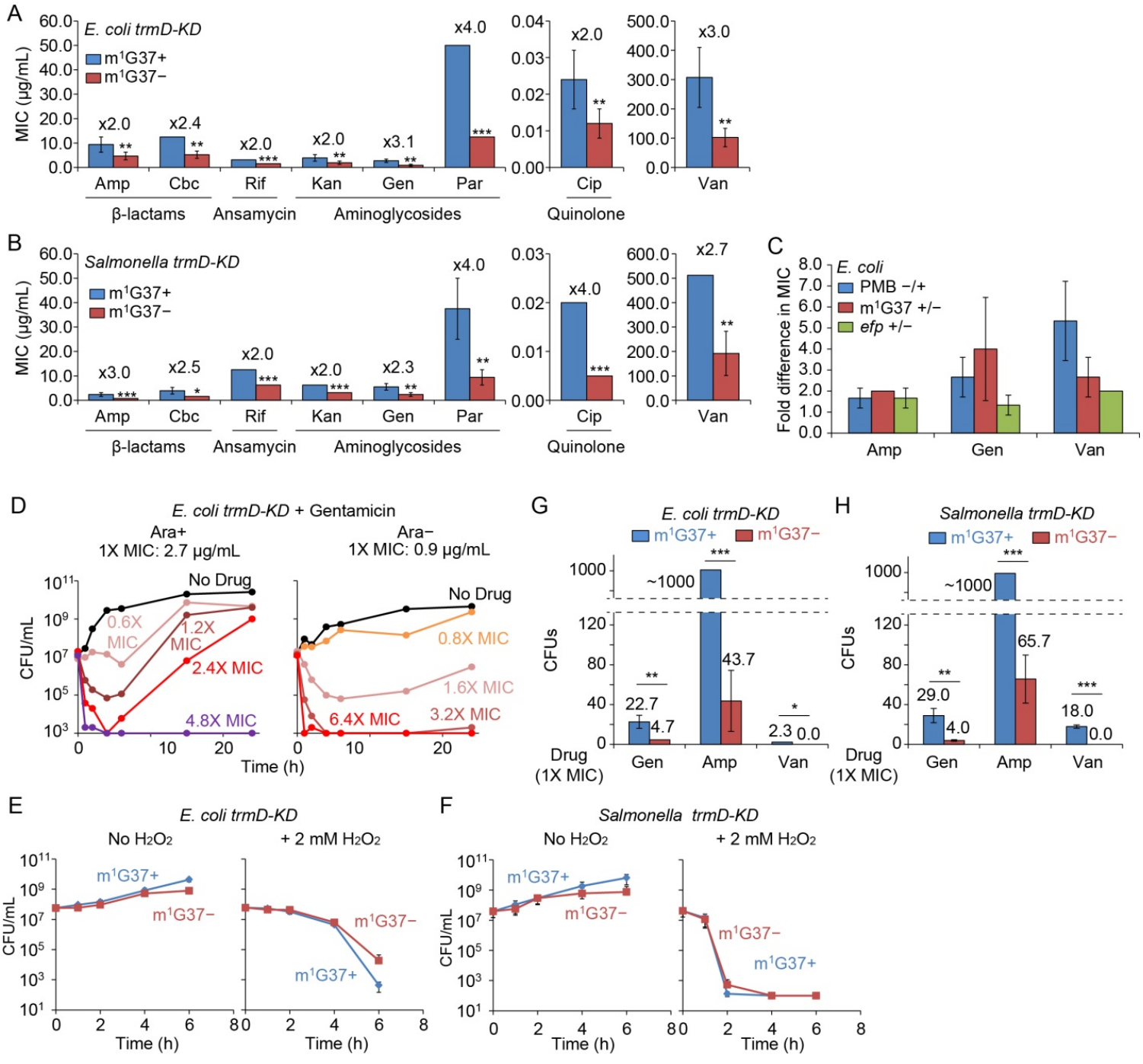


**Figure S6 (Related to Figure 4). *E. coli trmD-KD* cells are sensitized to antibiotics. (A and B)** The original antibiotic MIC values of *E. coli trmD-KD* (A) and *Salmonella trmD-KD* (B) cells under $m^1G37+$ (blue) and $m^1G37$-deficient (red) conditions used to generate Figure 4A, 4B. Error bars are SD from at least 3 independent experiments. "X" denotes the fold-change between $m^1G37+$ and $m^1G37$-deficient cells. Welch's *t*-test: $*p < 0.1$, $**p < 0.05$, $***p < 0.01$. Amp, ampicillin; Cbc, carbenicillin; Rif, rifampicin; Kan, kanamycin; Gen, gentamicin; Par, paromomycin; Cip, Ciprofloxacin; Van, vancomycin. $m^1G37-$ indicates $m^1G37$-deficient cells. **(C)** Comparison of the effect on MIC between polymyxin B, $m^1G37$-deficiency, and deletion of *efp*. EF-P is a translation factor that relieves ribosomes from stalling at consecutive proline codons and previous studies demonstrated its contribution to membrane integrity and antibiotic resistance (Navarre et al, 2010; Zou et al, 2012). MIC values of Amp, Gen, and Van were determined for *E. coli* BW25113 wild-type and Δ*efp* strains, and

the calculated MIC difference due to *efp* deletion (green) is shown along with those of polymyxin B (blue) and $m^1G37$ deficiency (red). **(D)** Time-kill plots of cell survival (CFU/mL) as a function of gentamicin concentration for *E. coli trmD-KD* cells in $m^1G37$+ (Ara+) or $m^1G37$-deficient (Ara−) conditions (n =1). Survival was lower in $m^1G37$-deficient cells than in $m^1G37$+ cells. *E. coli trmD-KD* cells were prepared as described in Figure 4C, 4D. **(E and F)** Time-kill plots of cell survival (CFU/mL) by oxidative stress. Overnight cultures of *E. coli trmD-KD* (E) and *Salmonella trmD-KD* (F) were pre-depleted as in time-kill assays (Figure 4C, 4D). Cells were then freshly inoculated into LB at $10^7$ CFU/mL with (blue) or without (red) 0.2% Ara and without (left) or with (right) 2 mM $H_2O_2$. At 0, 1, 2, 4, and 6 h after $H_2O_2$ treatment, 10-fold serial dilutions of cells were spotted on LB plates with 0.2% Ara to determine CFU/mL. $m^1G37-$ indicates $m^1G37$-deficient cells. **(G and H)** Resistance analysis of *trmD-KD* cells of *E. coli* (G) and *Salmonella* (H) against gentamicin, ampicillin, and vancomycin, with each drug tested at 1X MIC appropriate for $m^1G37$+ and $m^1G37$-deficient conditions. Resistance was more frequent by at least 5-fold for $m^1G37$+ relative to $m^1G37-$deficient cells in all cases ($n$ = 3).

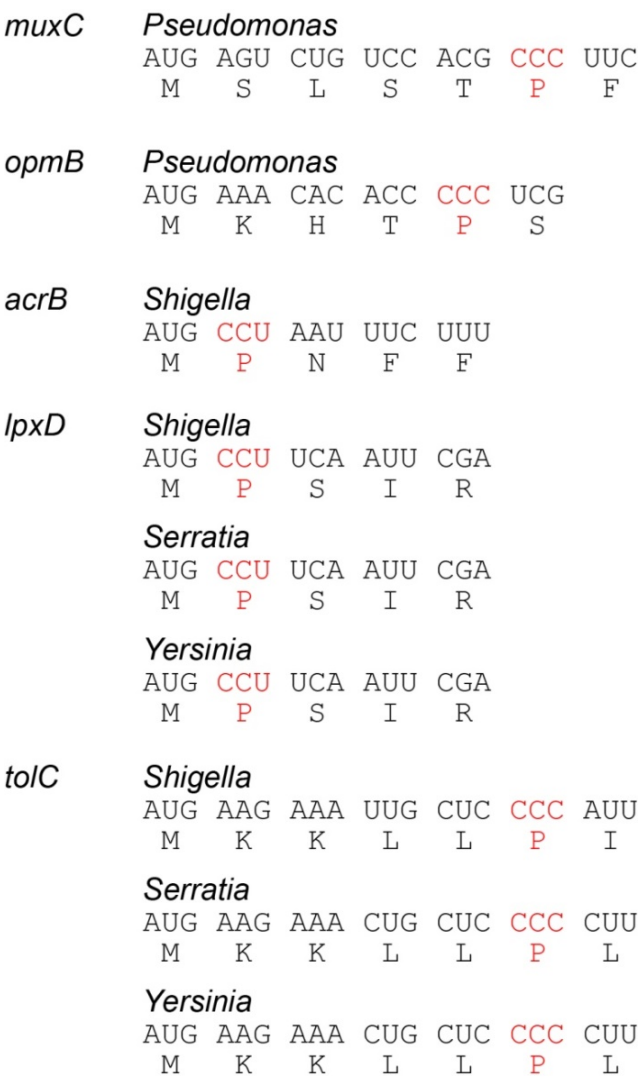


**Figure S7 (Related to Figure 7): Gram-negative pathogens contain CC[C/U] codons in membrane-associated genes.** Membrane-associated genes with CC[C/U] codons (red) near the start of each open reading frame are shown for *Pseudomonas aeruginosa, Shigella dysenteriae, Serratia marcescens,* and *Yersinia pestis*.